Impacts of gold nanoparticle exposure on two freshwater species: a phytoplanktonic alga (Scenedesmus subspicatus) and a benthic bivalve (Corbicula fluminea)

S. Renault[1], M. Baudrimont[1], N. Mesmer-Dudons[1], P. Gonzalez[1], S. Mornet[1] and A. Brisson[2]

[1] University Bordeaux 1, UMR-EPOC CNRS-5805, Geochemistry and Ecotoxicology of Metals in Aquatic systems team (GEMA)
[2] University Bordeaux 1, UMR-IECB CNRS-5471, Nanobiotechnology and Molecular Imaging Laboratory

Abstract

For years, nanotechnologies have developed the use of common materials, such as iron or silica, at an extremely small scale because of their new properties (reactivity, conductivity, optical sensitivity). More precisely, gold nanoparticles are used in numerous technologies such as electronics, new paints or research on cancer. But, despite their promising future and expansive utilization, only a few studies deal with their behaviors or impacts on the environment. Thus, we decided to explore the impacts of amine-coated 10nm gold nanoparticle (AuNp) contaminations on two freshwater aquatic models. The green alga *Scenedesmus subspicatus* was submitted to 24 h-direct exposures at four AuNp concentrations ($1.6x10^2$, $1.6x10^3$, $1.6x10^4$ and $1.6x10^5$ AuNp/cell) along with a control condition. The process used for the freshwater bivalves *Corbicula fluminea* was a trophic exposure during 7 days to three AuNp concentrations ($1.6x10^3$, $1.6x10^4$ and $1.6x10^5$ AuNp/cell). These conditions were tested in triplicate with controls. For these experiments, OD measurements (λ = 520nm) were performed to verify AuNp concentrations in the water (stability). Cell numerations of algae were used to determine the growth/mortality effects on this species. Cellular impacts and AuNp distributions in the two species were revealed by transmission electron microscopy (TEM). The bioaccumulation rates were assessed by gold dosages *via* MS-ICP procedures. Molecular impacts were analyzed by quantifications of metallothionein concentrations (metal detoxification protein) and genetic expressions *via* real-time RT-PCR. Our study focused on the expression of six genes encoding proteins involved in: metal detoxification (metallothionein), the response to oxidative stress (catalase and superoxide-dismutase), the mitochondrial respiratory chain (subunit 1 of the cytochrome-C-oxidase), the concentration of mitochondria (RNA12s) and the response to xenobiotics (glutathione S transferase); using the β-actin as reference of the basal rates of gene expressions.

The results showed a marked impact on the algae after a 24h-exposure to amine-coated 10nm gold nanoparticles, leading to 20% of mortality for the lowest contamination condition, while the highest one reached 50%. TEM examinations showed that AuNp were strongly adsorbed by the cell wall of algae, leading to progressive intracellular and wall disturbances. The bivalve contaminations revealed the ability of these particles to be bioaccumulated and to penetrate gills and digestive epithelia. Their lysosomial localization leads to the loss of their coating, which brought on an oxidative stress.

1 Introduction

Nanotechnology uses common materials such as iron, silica, titanium or cadmium [1, 2] at an extremely small scale to use their new physico-chemical properties [3]. The size of nanoparticles is included between 1 and 100nm. Their composition, form and size vary a lot along with their applications. In fact, nanoparticles are found everywhere as nanorods, nanospheres or nanotubes, in our computers, cosmetics and even in the air we breathe [1, 4]. However, despite their promising expansion, nanoparticle losses in the air, soils or more specifically in aquatic ecosystems have yet to be assessed. Despite the constant raise of their reliefs, studies dealing with their behaviors and potential impacts

on the environment are scarce [5, 6]. Moreover, considering the huge economic interest and the fast pace of research, human tests will soon be implemented and certainly before any ecotoxicological risk appraisal.

For a couple of centuries, gold has been considered as a noble and inert metal. Consequently, it was used in dentistry and in medicine for instance to alleviate arthritis [7]. But, in a recent past, gold nanoparticles have been used to explore their physic-chemical properties in order to finalize a new process of targeted tumor cell destructions. Gold nanoparticles are now used in a wide variety of newly developed technologies such as electronic components, new paints and covering [4]. At the nanometric scale, gold acquires novel spectroscopic and electromagnetic properties. For instance, these nanoparticles have an absorbency peak at 520 nm, due to the plasmonic resonance of surface gold atoms. For one specific size, their optical density is directly proportional to their concentration. Moreover, they are electronically dense due to their elevated extinction coefficient, allowing their detection by transmission electron microscopy [8]. To our knowledge and despite the known abilities of these particles coated with amined residues to enter the cells [5, 9, 10] and to maintain themselves soluble and stable in aqueous solution [6], the toxicological studies conducted on aquatic organisms are still scant.

In freshwater aquatic ecosystems, micro-algae represent the first targets for the fixation of chemical, metallic or organic pollutants. In fact, thanks to their presence in the suspended matter and to their elevated Surface/Volume ratio, these phytoplanktonic organisms can suffer from important direct contaminations. The green alga *Scenedesmus subspicatus* is commonly encountered in freshwater lakes and rivers. This species is notably used in French normalized ecotoxicological tests (AFNOR) to assess the potential growth inhibitory effect of new chemicals or effluents. Moreover, *S. subspicatus* can represent an important vector of trophic contamination due to its basal position in the trophic network. Bivalve mollusks such as *Corbicula fluminea* can also be directly and trophically contaminated by this kind of nanoparticles because of their important ventilatory activity for nutritional and respiratory purposes [11, 12, 13].

These are the reasons why we decided to explore the growth, cellular and molecular impacts of amine-coated 10nm gold nanoparticle (AuNp) contaminations on the green alga, *Scenedesmus subspicatus*, by a direct way, and on the freshwater bivalve, *Corbicula fluminea*, by a trophic way. The toxicological impacts were performed by cell numerations, transmission electron microscopy observations of the tissues, gold quantification in gills and digestive tract, genetic response analysis by real-time RT-PCR and detoxification evaluation by metallothionein (MT) concentration measurements. MTs are low molecular weight proteins which are able to sequester metallic ions thanks to their cystein residues' richness (30% of amino acids) [14]. This seclusion decreases metal's ability to exert their toxic effects on other cellular ligands. Moreover, MTs are inducible by oxidative stress also caused by metals.

The aim was then to investigate if the presence of AuNp in the cells could trigger a response of these proteins, either directly or by the generation of an oxidative stress. Therefore, we analyzed jointly the genetic expression of this protein and that of five other proteins involved in: the response to oxidative stress (catalase and superoxide-dismutase), the mitochondrial respiratory chain (subunit 1 of the cytochrome-C-oxidase), the concentration of mitochondria (RNA12s) and the response to xenobiotics (glutathione S transferase); using the β-actin as reference of the basal rates of gene expressions.

2   Materials and Methods

2.1   Gold nanoparticles

Gold nanoparticles (AuNp) used in these experiments were prepared by citrate reduction method optimised from the now classical protocol of Turkevich *et al.* [15], in order to obtain 10 nm diameter nanoparticles with a highly monodisperse size distribution. The procedure can be briefly described as follows: a volume of 400 mL of Milli-Q water is carried to boiling. 100 mL of an aqueous solution of 5.53 mM potassium tetrachloroaurate are added. The reaction medium is carried to the water reflux (110°C). The reduction of auric salts occurs upon addition of 50 mL of 3.4 mM sodium citrate dihydrate solution. The reaction is left 30 minutes to the water reflux and then cooled at room temperature. The average diameter measured by transmission electron microscopy is typically equal to 10.0 ± 0.5 nm (Fig. 1) and the concentration equal to 33 nM (1.964 10^{16} particles/L).

The gold surface functionalization based on the exchange of citrate ligand by a hetero-bifunctional PEO macromolecule bearing a thiol (-SH) group in ω position and amine (-NH2) group in α position was carried out following the method previously described [patent]. In few words, the coupling of PEO macromolecules can be summarized as follows. First, a homo-bifunctional bis-amino telechelic PEO is modified by thiolation of primary amines by 2 iminothiolane and second the thiolated macromolecules are coupled to the surface of the nanoparticles. The bis-amino telechelic PEO is dissolved in 0.1 M borate buffer at pH 8 in presence of 3 mM EDTA. After complete dissolution of the polymer, an equimolar aqueous solution of 2-iminothiolane is added. Then, after 4 hours of incubation, 10 equivalents of sodium borohydride are added in order to prevent the formation of disulphide bonds. The pH is adjusted to 6.5-7 with HCl. After 15 minutes of agitation (end of the gaseous emission), citrated gold nanoparticles are added in this medium under strong stirring. The number of moles of $(H_2N(CH_2)_3(OCH_2CH_2)_{34}O(CH_2)_3NHCHNH^+(CH_2)_3SH,Cl^-$ - Mw 1700g/mol) macromolecules corresponds at minimum to 12 times the equivalent number of moles of surface gold atoms guaranteeing the nanoparticle surface saturation by polymer chains. The nanoparticles were incubated in this medium overnight and protected from light. After reducing of the volume of the solution by rotary evaporator, the excess of hetero-bifunctional PEOs was eliminated by

centrifugation (25000 rpm namely 34000 g, 15 min, 4°C) using an ultracentrifuge (OptimaTM of Beckman Coulter™). Several cycles of washing with ultrapure water have to be carried out so that the maximum residual polymer concentration does not exceed 10^{-7} mol/L. At the last centrifugation, aminated gold nanoparticles are concentrated at least to 1.77 µM (1.068×10^{18} part/L) in ultrapure water, in order to avoid dilution of solutions used in the following experiments.

2.2   Biological models

Scenedesmus subspicatus is a green freshwater micro-alga commonly found in lakes and rivers [16]. This unicellular alga belongs to the chlorophycea family and is currently used in aquatic ecotoxicological normalized tests on pesticide toxicity.

Corbicula fluminea is a freshwater clam which arrived in France during the 80's from the United States, but originated from Japan [17]. It is an invasive species which is well studied by ecotoxicologists as regards metal bioaccumulations.

2.3   Direct exposure of *S. scenedesmus*

A growing cell culture was chosen in the breeding lab and daily numerated using a Nageotte cell. A volume of this culture was centrifuged and cells were diluted with urban freshwater (Talence, France) to obtain a new solution of 30×10^6 cells/ml. 20ml of this solution were set in five polypropylene tubes (50ml of capacity) and contaminated with five concentrations of AuNp without reply: 0 AuNp/cell as negative control, 1.6×10^2 AuNp/cell (Npx0.01), 1.6×10^3 AuNp/cell (Npx0.1), 1.6×10^4 AuNp/cell (Npx1) and 1.6×10^5 AuNp/cell (Npx10). The experiment length was 24h with an orbital rotation as agitation, and 12h of continuous lighting.

2.4   Trophic exposure of *C. fluminea*

Thirty-six *C. fluminea* were calibrated at 19 ± 1 mm of the maximal shell length. No food was supplied during seven days before the start of the experiments to ensure active ventilation and digestion during the trophic contamination periods. Then, two bivalves were placed in experimental units constituted of polypropylene flasks containing 40 ml of a suspended solution of green algae (10^6 cells/ml) prepared in Talence urban freshwater permanently supplied with oxygen by a catheter, and maintained at 15°C in an air-conditioned room for one week. The chosen alga concentration (10^6 cells/ml) is not likely to modify the ventilation activity of the bivalves [13]. Moreover, algae were maintained in suspension by constant agitation of the water *via* a magnetic rotator. The experiments were conducted in two times. First, we tested low and medium concentrations (Npx0.1 and Npx1) because of their limited mortality impact on algae. And in the second time, we wanted to substitute a highest (Npx10) for the lowest concentration (Npx0.1) despite the huge mortality induced on algae. Three replicates of each contamination condition (control included) were conducted.

2.5   MS-ICP sample preparation

To assess AuNp bioaccumulation rates in bivalves, gold dosages were executed by MS-ICP (Mass Spectrometry – Inductively Coupled Plasma) processes by the Talence's GEMA team as described in Schäfer *et al*., 2006 [18], on mineralized gills and visceral mass (containing the digestive tract, the digestive glands, the stomach, the gonads…) of each bivalve. In fact, after dissection and storage at -80°C, gills and visceral mass were weighted, immersed in high concentrated nitric acid (65%), heated three hours at 100°C and diluted in demineralized water to obtain mineralized samples.

Table 1

Accession numbers and specific primers pairs used in the quantitative PCR analysis of the seven studied genes of C. fluminea *([a]: forward primer, [b]: reverse primer)*

| Gene name	Accession number	Specific primers (5'-3')
β-actin	EF446608	CCTTTACCACAACAGCCGA [a] AGCATAGCCTCAGGGCA [b]
cat	EF446609	CCTTCAGTGCGTAGTCTGG [a] CCTGTTCTCTGACCGTGG [b]
cox1	AF120666	GTTGAGAGTGGTGCTGGG [a] TGTAGTCCGAATTAGCTTTTGCG [b]
gst	EF446610	GCCAGGCTATCCGCTATCT [a] TGTCCACCTTTAGGGCCTC [b]
mt	EF185126	CGGCTATCTCCCGCGA [a] AGCTTTTACCAGAACCAAACAGT [b]
sodMn	EF446611	CTGTAGGTAGTAAGCGTGCTCC [a] GGATCATTTGACGAGATGAAGGC [b]
RNA12s	EF44661	AGCATTACTATGTTACGACTTACCTCA [a] AGTTCAGGTAGACGTGTAGGG [b]
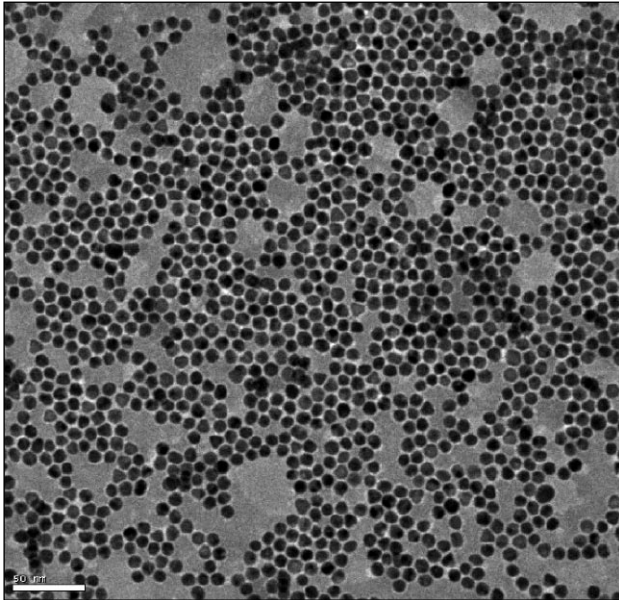
Figure 1

TEM observation of amine-coated 10nm gold nanoparticles obtained by the optimized Turkewich method

Figure 2

520nm OD measurements of the AuNp solutions made with different kind of freshwater (Arcachon's water 1 and 2 are two replicates of the same sample)

2.6 Alga concentration measurements

The growth impact of AuNp on *S. subspicatus* was tracked by cell numerations on Nageotte cell to determine the cell concentrations after 0, 6, 12 and 24h of contamination, by sampling each time 100µl.

2.7 Transmission electron microscopy examinations

AuNp cellular distribution and impacts were revealed using transmission electron microscopy since these particles have a high extinction coefficient making them impenetrable to electrons. Thus, at the end of the experiment, the bivalves were dissected (foot removed) and placed in a fixing solution of glutaraldehyde (2%) and cacodylate buffer (0,05M) for 24H at 4°C. Alga cells were picked out by centrifugation (5mn at 3000g, 20°C) and dissolved in the same fixing solution for 24H at 4°C. The fixed bivalves and alga cells were then washed three times using a solution of cacodylate buffer (0,05M) and NaCl (1%). Algae were recovered by centrifugation and included in agar gels. Bivalves and gels were placed in a post-fixing solution of osmium tetroxyde (1%) and cacodylate buffer (0,05M) for 2H and dried with increasing concentrations of ethanol and propylene oxide. Then, they were dipped into resin solutions (araldite) of increasing concentrations, embedded in pure resin and heated at 60°C for 3 days (resin polymerization). Finally, semi and ultrathin sections (1.5 and 0.6µm) were cut with an ultramicrotom, using glass and diamond knives. Semi thin sections were dyed for 1 or 2 minutes with a solution of azur blue II and observed under a light microscope. Ultrathin sections were placed on copper grids, contrasted for 10 minutes in solution of uranyl acetate (5%) and 3 minutes in a solution of lead citrate (pH 9) and observed, using a transmission electron microscope (TEM Philips CM120).
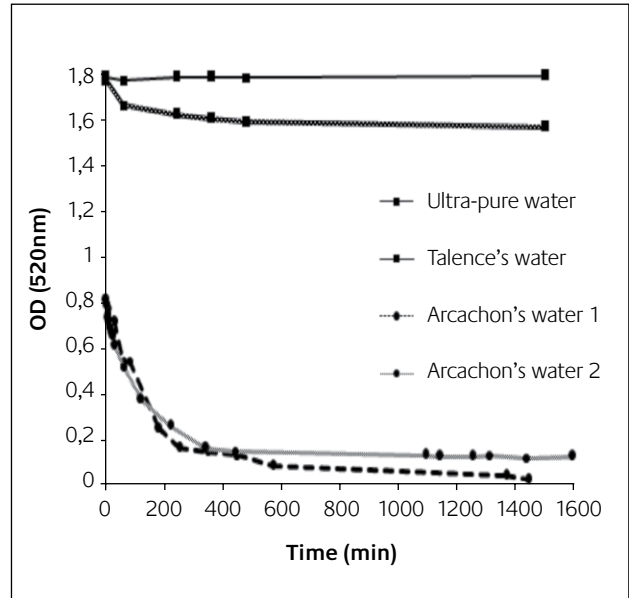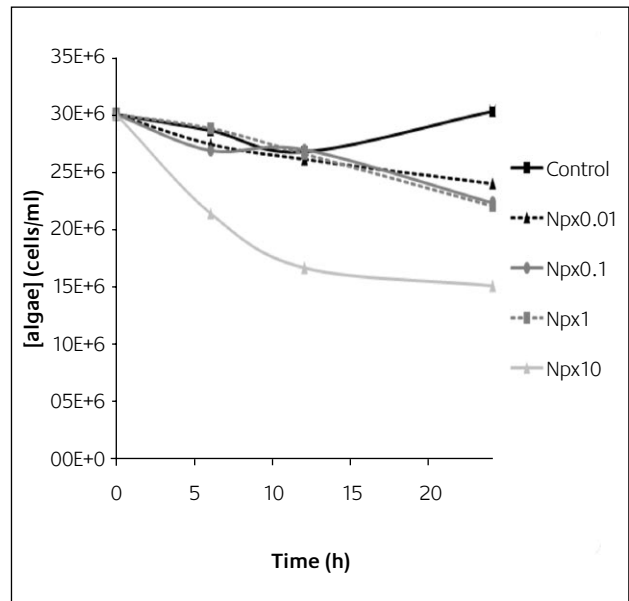

Figure 3

S. subpicatus concentrations for each AuNp concentrations during the direct exposure, 0, 6, 12 and 24h after the beginning of the experiment (Npx0.01=1.6x10² AuNp/cell; Npx0.1=1.6x10³ AuNp/cell; Npx1=1.6x10⁴ AuNp/cell; Npx10=1.6x10⁵ AuNp/cell)

2.8 Metallothionein concentration measurements

Thanks to their numerous cystein residues, MTs interact with metallic ions in order to protect cells against them. This peculiarity is used to measure their concentration. After dissection and storage at -80°C in a saturated nitrogen atmosphere, gills and visceral mass were weighted, immersed in Tris buffer (25mM) and ground on ice in a saturated nitrogen atmosphere. Blended samples were centrifuged (20,000g) for 1 hour at 4°C. 200µl of supernatants,
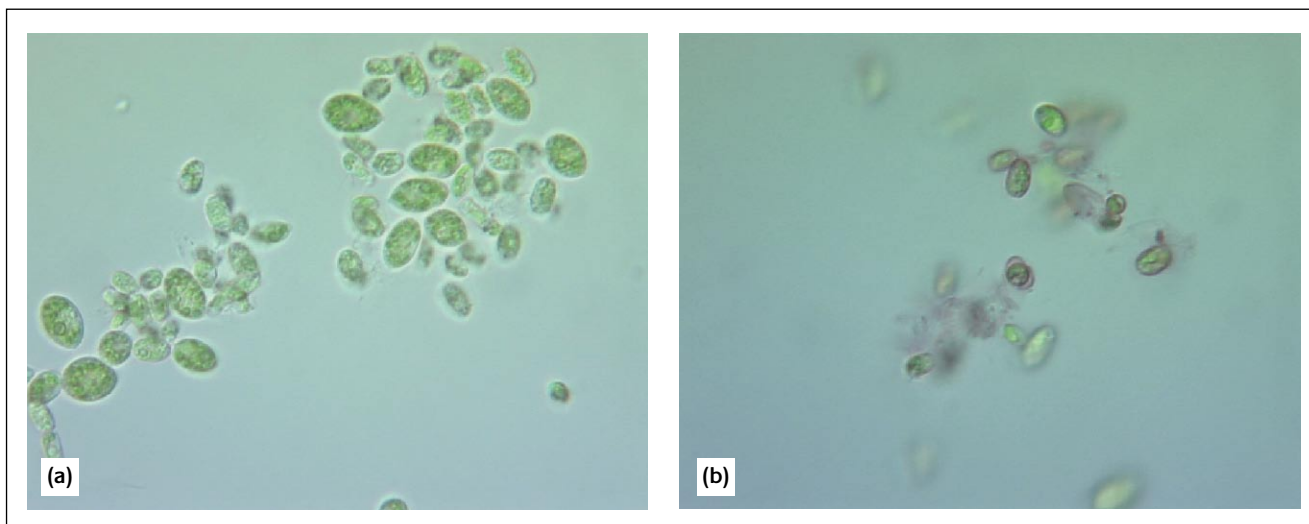
Figure 4
Direct observations of suspended algae S. subspicatus *(a: control and b: Npx10; original magnification: x63)*

containing low molecular weight proteins, were withheld and saturated by adding 200µl of a highly concentrated solution of mercury (50mg/l in TCA 10%). Remainder mercury (not fixed to MTs) was then segregated by the addition of a porcine hemoglobin solution and centrifugation (20min at 20,000g; 20°C). Supernatants were weighed and 100µl were withheld to measure mercury concentration by atomic absorption spectrometry (Leco AMA 254), as described in Legeay *et al.*, 2005 [19].

2.9 Genetic expression analysis

The expression of the 6 retained genes (*cat, cox1, gst, mt1, sodMn* and *12s*) was measured by quantitative real-time RT-PCR (Reverse transcription-Polymerase Chain Reaction), using the β-actine gene expression as referral. Total RNAs were extracted from 40 mg of gills and visceral mass, stored in 500µl of "RNA later" buffer (Quiagen) at -80°C, using the Absolutely RNA RT-PCR Miniprep kit (Stratagene), according to the manufacturer's instructions. First-strand cDNA was synthesized from 5 µg total RNA using the Stratascript First-Strand Synthesis System (Stratagene) according to the manufacturer's instructions. The cDNA mixture was conserved at −20°C until it was required for use in real-time PCR reaction. The accession numbers of the 7 used genes are reported in Table 1. For each gene, specific primer pairs were determined using the LightCycler probe design software (version 1.0, Roche). All these primer pairs are reported in Table 1.

Amplification of cDNA was monitored using the DNA intercaling dye SyberGreen I. Real-time PCR reactions were performed in a LightCycler (Roche) following the manufacturer's instructions (one cycle at 95°C for 10 min, and 50 amplification cycles at 95°C for 5s, 60°C for 5s and 72°C for 20s). Each 20 µl reaction contained 2 µl of reverse transcribed product template, 1 µl of master mix including the SyberGreen I fluorescent dye (Roche), and the gene-specific primer pair at a final concentration of 300 nM for each primer. Reaction specificity was determined for each reaction from the dissociation curve of the PCR product. This dissociation curve was obtained by following the SyberGreen fluorescence level during a gradual heating of the PCR products from 60 to 95 °C. Relative quantification of each gene expression level was normalized according to the actin gene expression.

3 Results

3.1 Nanoparticle stability in aqueous solution

Before any ecotoxicological experiments, we wanted to be acquainted with the stability of the amine-coated 10nm gold nanoparticles in aqueous solutions. Optic density measurements (520nm) were carried out with urban freshwater from two different origins and with ultrapure water. Some micro-liters of our AuNp solution were just diluted in each kind of water and the OD's (520nm) kinetic evolution was measured.

As shown figure 2, ultrapure water OD did not change during the test and that of Talence's water decreased slightly at the beginning but remained constant and high (about 1.6). On the contrary, the OD of Arcachon's waters decreased strongly for the first 4h and remained constant and very low until the end of the test (less than 0.1). Siliceous concentrations of Talence's and Arcachon's waters were assessed but did not explain these results.

3.2 Direct contamination of algae

3.2.1 Growth inhibition
As shown figure 3, all contaminated units displayed a decrease in their cell concentrations while the control unit resumed growth after the first 12h of the experiment. However, the cell concentration of the most contaminated unit (Npx10) decrease more brutally (40% of mortality after 12h) than the others (Npx0.01, Npx0.1, Npx1) which had the same decreasing outline and reached only 20-26% of mortality. Last but not least, the lethal dose of 50% (LD_{50}) was reached after a 24h exposure to $1.6x10^5$AuNp/cell (Npx10).
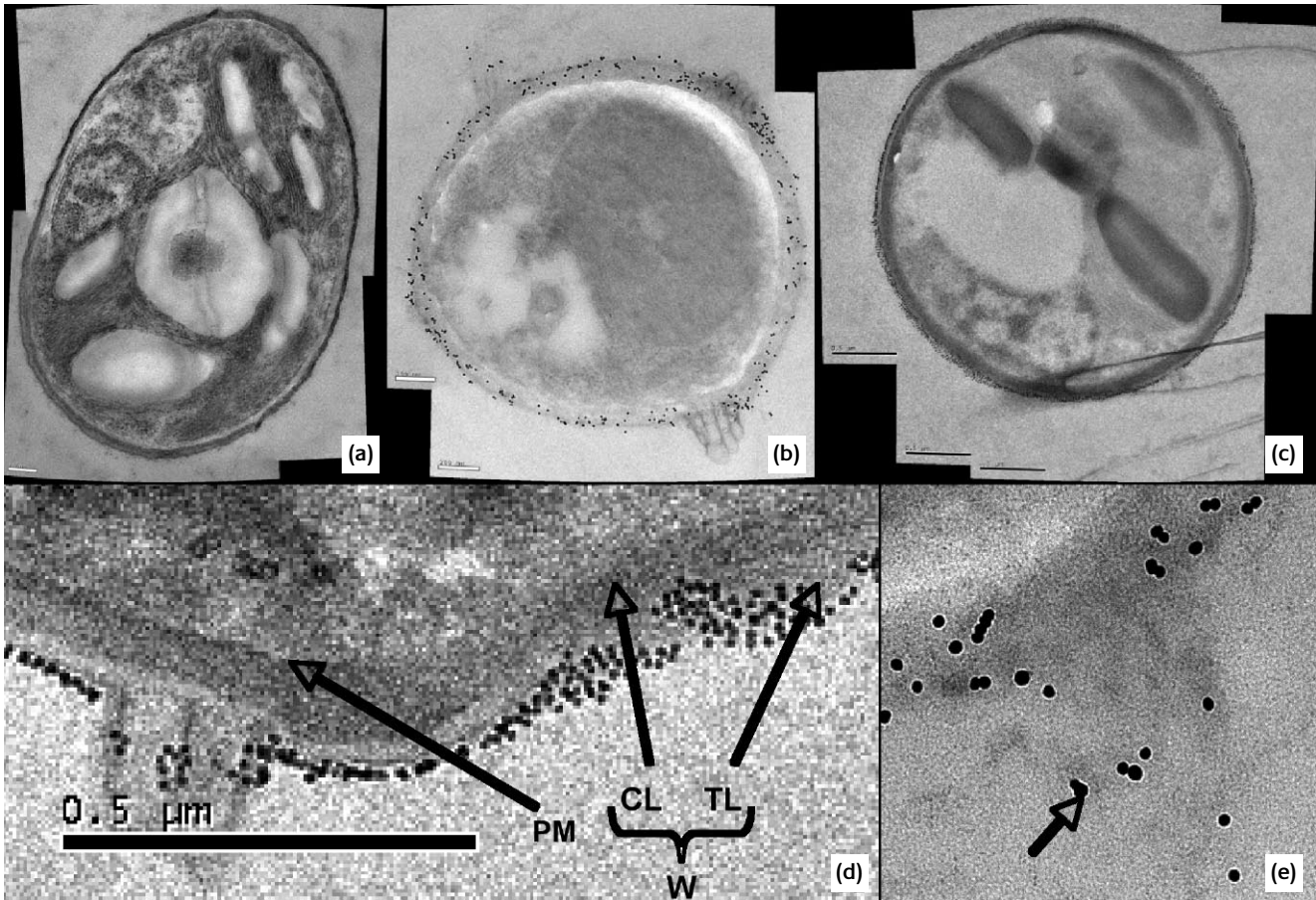
Figure 5

TEM observations of ultra-thin slices of S. subspicatus *(a: control; b and e: Npx1; c and d: Npx10; CL: cellulosic layer, PM: plasmic membrane, TL: trilaminar layer and W: cell wall; e: the arrow shows a 17nm AuNp)*

3.2.2 Microscopic examinations

3.2.2.1 Light microscopy

Examinations of cell solutions were done by light microscopy to detect AuNp impacts on the broad aspect of alga cells. The control and the less contaminated units contained a lot of colonies (Fig. 4 a), which means a good growth by cell division [20]. Conversely, the other contaminated units (Npx0.1 to Npx10) contained a few of colonies and cell walls were tinctured (Fig. 4 b). These pink tinctures, which were increasing at the same pace as the AuNp concentrations, were due to the presence of AuNp around the cell walls. Moreover, emptied cells and cell rubbles were found in the two most contaminated units (Npx1 and Npx10). Thin slices of cells were examined to evaluate AuNp impact on the alga cell dimension and revealed a significant decrease of the contaminated cells' dimension (data not shown).

3.2.2.2 Transmission electron microscopy

Ultra-thin sections were examined by transmission electron microscopy in order to bring to light the process of AuNp toxicity. Control algae had a neat shape with well delineated organits (Fig. 5 a) while the most contaminated algae (Npx1 and Npx10) showed cell suffering clues and lots of AuNp adsorbed on the cell wall (Fig. 5 b and c). Moreover, a zoom in on the cell wall showed that AuNp could penetrate the trilaminar layer to be adsorbed on the cellulosic layer (Fig. 5 d). Even so, not a single AuNp could be observed inside

the cells and those which had penetrated the cellulosic layer agglutinated in bigger wads (Fig. 5 e, AuNp arrowed: 17nm).

3.3 Trophic contamination of bivalves

3.3.1 Microscopic examinations

Examinations of stomach contents showed that whole ingested algae were digested at the end of the experiments. Targeted organs for the microscopic observations were the gills and the digestive tract since in filter organisms they are the first organs in contact with toxic elements. TEM examinations did not reveal any structural disturbance of branchial and digestive tissues. However, they demonstrated the ability of AuNp to penetrate those epithelia.

During the first part of the experiment, AuNp were detected close to apical lashes of the stomach epithelia, inside those cells (Fig. 6 a) and in their nucleus. Even if some AuNp were observed near the basal side of epithelial stomach cells, no particles could be detected beyond those cells. Contrarily to AuNp found in stomachic cells, those detected in gills were neither located in cytoplasm nor in nuclei but only in lysosomial vesicles (Fig. 6 b). Moreover, this kind of vesicles was less numerous in controls than in contaminated gill cells.

In the second part of the experiment, AuNp detected in gills remained localized in lysosomial vesicles while those of the digestive tract were not located in cytoplasm or nuclei of
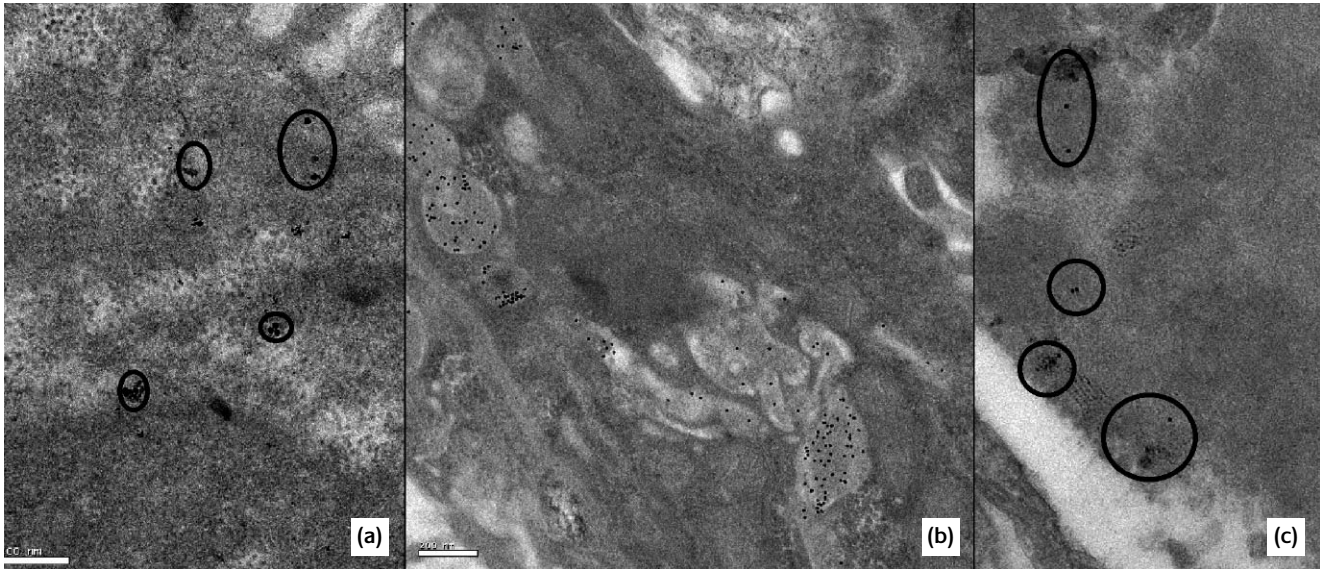
Figure 6

TEM observations of ultra-thin slices of contaminated C. fluminea *(a: epithelial stomachic cell Npx1, b: epithelial branchial cell Npx10, and c: epithelial cell of the digestive gland Npx1; circles surround AuNp)*

stomach cells any more, but in the digestive vacuole of the digestive gland cells (Fig. 6 c).

Ultra-thin slices of kidney were examined in order to know whether AuNp are able to cross the digestive barrier, move in hemolymph and be filtered by kidneys. But, for one week of the highest contamination, not a single AuNp was found in kidneys.

3.3.2 Gold concentrations

Gold concentrations measured in gills and the visceral mass of the controls were lower than the detection limit of the machine. Thus data were rounded to 0 and could not be statistically compared to those of the contaminated mollusks. Even so, gold concentrations of the low contaminated bivalves (Npx0.1) were significantly different from those of the moderately contaminated gills (Npx1) or digestive tracts (fig. 7), reaching respectively 0.8 and 4.3 µg/g (fw).

3.3.3 Metallothionein concentrations

On the one hand, weakly and moderately contaminated bivalves (Npx0.1 and Npx1 a) showed concentrations statistically equivalent to controls (Fig. 8; control a). On the other hand, metallothionein concentrations increased sharply in the gills and visceral mass of highly contaminated bivalves (Npx10) compared to controls (control b). The induction factors were respectively 3.13 and 2.96. Last but not least, metallothionein concentrations measured in those bivalves reached 110 nmol site Hg/g (fw) in the visceral mass.

3.3.4 Genetic expression quantification

Induction factors of the six analyzed genes were calculated in relation with control rates and grouped in table 2. Lowest contaminated bivalves (Npx0.1) did not show any discrepancy of genetic expression in gills and visceral mass. Instead, the presence of AuNp in gills of moderately contaminated mollusks (Npx1a)
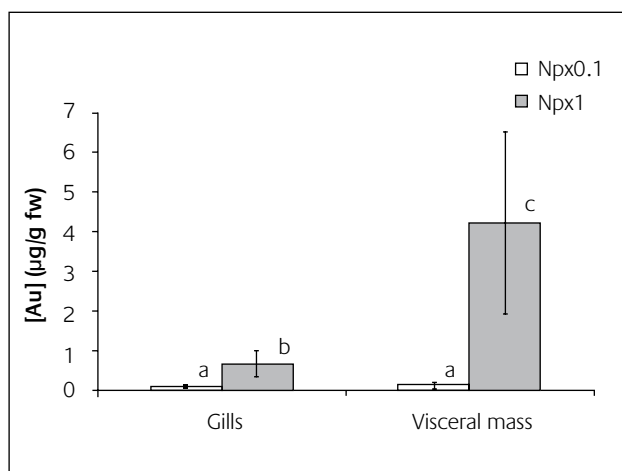

Figure 7

Gold concentrations in gills and visceral mass of C. fluminea *from the first part of the trophic experiment (letters show significant mean differences according to the Student test, with n=3 and p<0.05)*

Table 2

Expression's factors of the six genes studied in C. fluminea *compared to the basal level of the controls (>1: induction, <1: repression and /: statistically equal to control).*

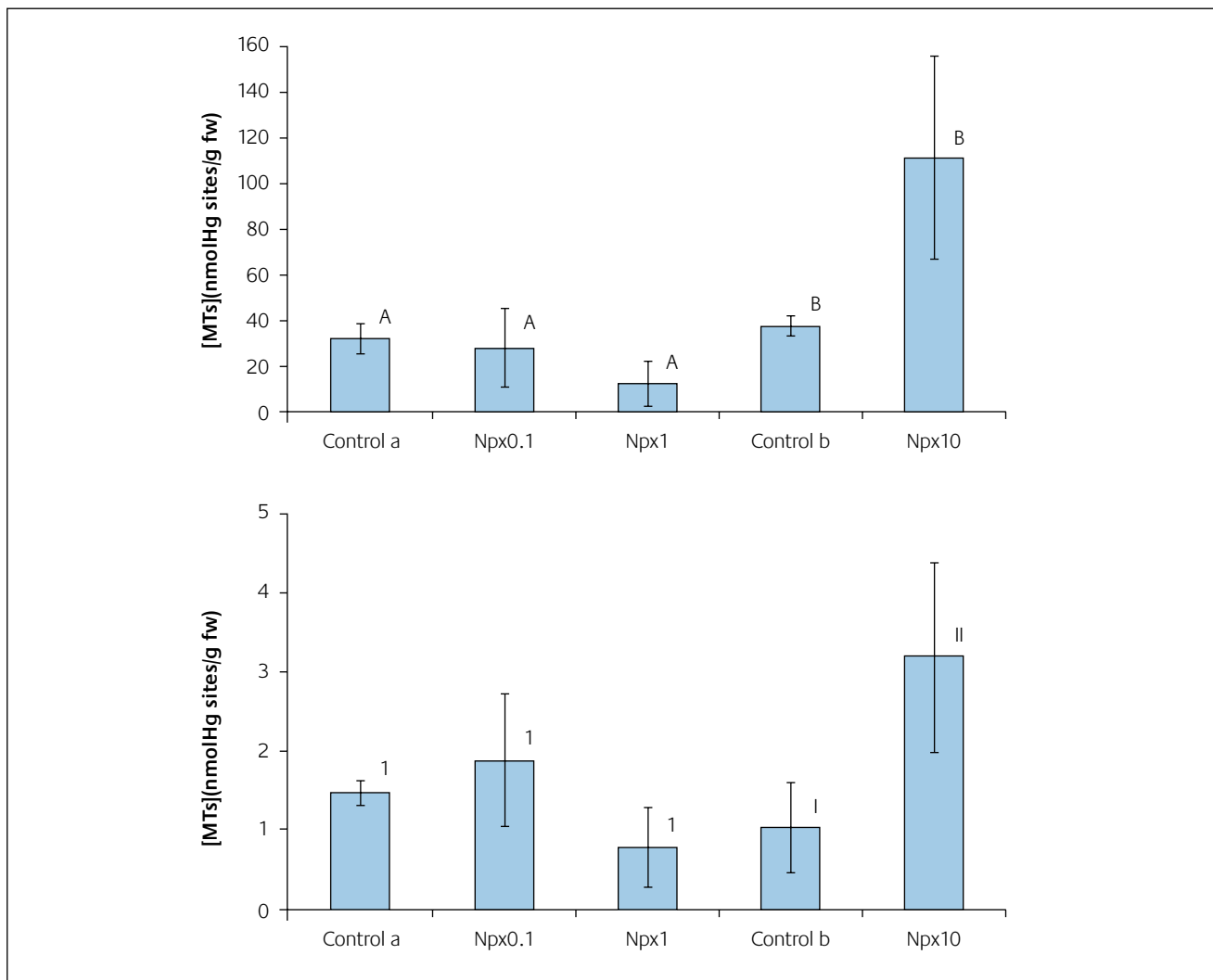|	Genes/ Conditions	Npx0.1	Npx1a	Npx1b	Npx10
Gills	cat	/	/	/	/
	sodMn	/	3	1/3	/
	gst	/	/	1/3	1/3
	mt1	/	4	/	/
	cox1	/	/	1/2	/
	RNA12s	/	/	/	/
Visceral mass	cat	/	/	31	12
	sodMn	/	/	/	/
	gst	/	/	/	/
	mt1	/	/	/	/
	cox1	/	/	/	/
	RNA12s	/	/	/	/

Figure 8
Metallothionein concentrations in visceral mass and gills of C. fluminea *from the two parts of the trophic experiment (a: visceral mass and b: gills) (letters and numbers show significant mean differences according to the Student test, with n=3 and p<0.05)*

caused an expression induction of metallothionein (x4) and superoxide dismutase genes (x3).

On the other hand, during the second part of the experiment, the presence of the AuNp caused significant repressions of the superoxide dismutase (x1/3), glutathion S transferase (x1/3) and cytochrome C oxidase (x1/2) gene expressions in gills and inductions of the catalase gene (x31) in visceral mass of moderately contaminated bivalves (Npx1 b). The repression of the gst gene (x1/3) and the induction of the catalase gene (x12) were maintained in the most contaminated bivalves (Npx10).

4   Discussion

4.1   Alga mortality
High mortality rates happened during the direct exposure of algae to amine-coated 10nm gold nanoparticles. The lethal dose of 50% was reached after a 24h exposure to $1.6x10^5$AuNp/cell. Even so, since the contaminated units

Npx0.1 to Npx1 followed the same mortality outline, the impact of AuNp on *S. subspicatus* do not seem to respect a dose effect. Microscopic examinations of contaminated algae revealed that not a single AuNp could be found inside the cells. Thus, AuNp did not kill algae by penetration but by smothering and weakening the cell wall. Indeed, AuNp have been observed all around the wall of contaminated cells, which coming along suffering clues such as the decreasing size. Moreover, AuNp were detected in the trilaminar layer and on the cellulosic layer of the cell wall. This adsorption is due to electrostatic attractions between the negatively charged cell walls [21, 22] and the positively charged amines coating the AuNp [8, 21]. Then, AuNp clusters observed in the wall made it dysfunctional, maybe because of interactions between AuNp and the cell wall components. But, the trilaminar layer, essentially composed of non hydrolysable poly-unsaturated fatty acids [22], is in charge of the structural integrity and the resistance of the cell against the hydraulic pressure [23, 24]. So, alga mortalities may have been caused by the disturbance of the cell wall and the vital exchanges which occur there. Several studies are in agreement with our results since they

have shown that gold nanoparticles exert toxicity against human red corpuscles and the bacteria *Escherichia coli* by their adsorption while that of amine-coated gold nanoparticles is due to the degree of surface charges [25]. However, other studies seem to indicate that polyethylene glycol coatings can be more toxic than nanoparticles [26, 27].

4.2   Cellular localizations and impacts in bivalves

Examinations of the digestive contents of bivalves showed that algae were ingested and digested at the end of the experiments. Thus, mollusks were quite contaminated by AuNp by a trophic way. Secondly, amine-coated 10nm gold nanoparticles were detected inside branchial and digestive cells, so they are able to penetrate the branchial and digestive barriers of *C. fluminea*. Even so, AuNp had various cellular localizations inside the digestive tract cells. In the first part of the experiment, AuNp had penetrated the stomach cells without any preferential distribution (cytoplasm, nucleus), while in the second part, AuNp did not enter the stomach cells but the epithelial cells of the digestive glands and were only localized in lysosomial vesicles. This discrepancy of histological and cellular distributions may be due to a fluctuation in the digestive speed and intensity. In the first time, the extra-cellular stomach digestion [28, 29] may have been slower than in the second time. So, in the first part, AuNp could penetrate stomach cells while they were conveyed with nutrients to digestive gland cells (intracellular digestion) in the second one. Thus, the bivalve's metabolism seems to play an important role in AuNp toxic impacts.

On the other hand, in the first part of the experiment as well as in the second, AuNp had penetrated branchial cells and their localizations were identical. AuNp were detected in special cellular structures indentified as vesicles. But, these vesicles could not be observed at the same level in control branchial cells. So, there construction seems to be linked to the presence of AuNp inside the cells. Even so, as the AuNp's enter process could not be observed, it still remains to be established whether these vesicles are the cause or the effect of the AuNp's penetration. Thus, if AuNp were endocytated or pinocytated, the vesicles were constructed by the invagination and parting of the plasmic membrane and transported into the cytoplasm. If AuNp penetrated cells via diffusion or mediated by conveyors or transmembrane channels, vesicle genesis could be a defensive device aiming to protect cells by AuNp sequestration. Several studies are in agreement with these conclusions and show that AuNp are able to penetrate human leucocytes *via* endocytose process [9] and that they are localized in lysosomial vesicles after penetration of macrophages [10]. Moreover, epithelial cells of *C. fluminea* are able to generate lysosomial vesicles in response to a metal contamination [28].

4.3   Bioaccumulation in bivalves

MS-ICP measurements of gold concentrations in bivalves' gills and visceral mass were done in order to look over the microscopic examinations which showed the presence of gold in these organs, and to assess the bioaccumulation rates in *C. fluminea*. Gold presence could be certified in weakly and moderately contaminated mollusks since their gold contents were significantly higher than those of controls. Moreover, bioconcentration factors up to 4,000 and 26,000 were calculated from gold concentrations in gills and visceral mass of the moderately contaminated bivalves.

4.4   Bivalve's molecular impacts

4.4.1 Gills

On the one hand, the lowest contaminated bivalves (Npx0.1) did not show any difference in the genetic expressions of the six genes studied when compared to those of the controls. This is in agreement with histological examinations and gold analyses since only few nanoparticles were detected in these organisms.

On the other hand, expression inductions and repressions were found in moderately contaminated mollusks (Npx1). In fact, in the first part of the experiment, the expression of the *mt1* and the *sodMn* genes were induced significantly. The SODMn proteins are known to be over-expressed during an oxidative stress [30, 31] since they reduce superoxide ions into lower toxic elements. Moreover, it has been demonstrated that metallothioneins are able, *via* thiol-functions, to seclude seven divalent-metallic ions in mammalian cells [32] and that their gene's promoter contains several regulator element (MRE) reacting to metallically-activated transcription factors (MTF-1) [33]. Thus, the presence of gold nanoparticles in branchial cells has brought on an oxidative stress. Even so, it was not possible to know whether the gold effect is linked to nanoparticles or gold ions. Indeed, it has been shown that, in extremely acid conditions, Au(0) could be oxidized into Au(III) which gives toxic gold salts (AuCl$_4^-$) [34]. Moreover, AuNp detected in gills were localized in lysosomial vesicles where pH is low. Nevertheless, lysosomial pH did not seem to be low enough to entirely fade nanoparticles but just enough to pick up nanoparticle's coatings. In this case, the oxidative stress and the expression inductions of *mt1* and *sodMn* genes may not have been provoked by gold ions but by free gold nanoparticles. However, the proteic metallothionein rates in these bivalves were equivalent to those of the controls. This is amazing since when genetic expression is induced, a proteic raise is expected. Nevertheless, it has been demonstrated that a temporal gap could happen between the time of genetic expression and the time of protein production of metallothioneins in zebra-fish *Danio rerio* [31].

In parallel, in the second part of the experiment, significant repressions of the *gst*, the *cox1* and the *sodMn* genes were unveiled in gills of moderately contaminated bivalves (Npx1 b) while a great amount of AuNp was observed. However, the repression of *cox1* expression hints to a slowed-mitochondrial activity linked to a decrease of the respiratory rate. But, mitochondria represent the major spot of reactive oxygen species' production. In all likelihood, bivalves of the second

part of the experiment must have had faster ventilatory and digestive activities than those of the first part. Thus, after algae ingestion and digestion, these mollusks had slowed their metabolism to get ready for another fast period. In this case, it is possible that the occurrence of the oxidative stress was too premature to be detected.

In the case of highly contaminated bivalves (Npx10), only the *gst* expression was modified compared to the controls. GST proteins are expected to be produced in presence of xenobiotics, but gst gene's expression was repressed in presence of AuNp. Moreover, metallothionein concentrations in these organs were greatly higher than in the controls while their gene expression remained constant. There again, these results can be explained by the temporal gap between gene expression and protein production. Indeed, when protein rates are higher in contaminated organisms than in controls, it means that their gene expression was induced and got back to its basal level *via* an auto-regulator system. It has been shown that MTs play an important role in metal detoxification in the bivalve *C. fluminea*, since they are in charge of the sequestration of metal ions [12]. Thus, the oxidative stress previously mentioned could have been provoked by the presence of gold and abolished by a massive production of MTs which could have protected the cells against metallically-induced oxidative stress.

4.4.2 Visceral mass

Visceral mass of weakly and moderately contaminated bivalves of the first part of the experiment (Npx0.1 and Npx1 a) did not show any difference in the genetic expressions of the six genes studied while their gold concentrations were higher than in gills. It can be explained by two phenomena: i) in the visceral mass, the basal level of genetic expression is higher than in gills, so it needs a bigger stress to activate the genetic responses; ii) AuNp were localized in cytoplasm and nuclei, so they did not lose their coating and stayed inert. On the contrary, in the second part of the experiment, significant inductions of the catalase gene could be observed in moderately and highly contaminated bivalves (Npx1 b and Npx10). It can be explained by the emergence of an oxidative stress due to the presence of hydrogen peroxides [30]. Moreover, MT concentrations of highly contaminated mollusks reached the value of 110 nmol of fixed Hg/g of fresh weight which have not been measured yet in this species, even after 5 months of transplantation in a highly contaminated area [11, 35]. This result seems to suggest that the amine-coated 10nm gold nanoparticles have a strong impact from 7 days of trophic exposure.

5. Conclusion

This study has shown the considerable toxicity of amine-coated 10nm gold nanoparticles against the green freshwater micro-alga *Scenedesmus subspicatus*. The lethal dose for 50% of the population has been reached with a 24h-exposure at 1.6×10^5 AuNp/cell. Moreover, their toxicity seems to be linked to their adsorption and disturbance of the cell wall. Besides, it has been demonstrated that those particles are able to penetrate and be bioaccumulated in branchial and digestive epithelial cells of the freshwater bivalve *Corbicula fluminea* during a trophic contamination experiment. At last, it has been revealed that they can trigger the MT's overproduction and an oxidative stress in gills and the visceral mass of this species.

As this report is one of the first to deal with amine-coated 10nm gold nanoparticle toxicity in aquatic systems, much more experiments are needed to strengthen the results. But in a larger view, it is important to establish precisely their concentrations and behaviors in these ecosystems and to study their toxicological and ecotoxicological risks, mostly linked to their size [36, 37], composition (carbonated, siliceous, metallic...), shape (nanospheres, nanorods, nanotubes...) and coating (polyethylene glycol, cetyltrimethylammonium bromide...) diversity.

Sophie RENAULT is a PhD student who works on the "Eco-toxicological study of the metallic contamination of European eels living in the Gironde estuary" in the context of the National Research Agency's program: EEL-scope. She received her Masters in Ecological Systems at the University Bordeaux 1 while she worked on the toxicity of gold nanoparticles on aquatic organisms at the physiological, biochemical and genetic scales.

Magalie BAUDRIMONT received her PhD in Ecotoxicology at the University Bordeaux 1 in 1997. She is currently Associate Professor from the University Bordeaux 1 at the Marine Station of Arcachon. Her research concerns the cellular mechanisms of metals detoxification and the adaptative response of aquatic organisms at the physiological, biochemical and genetic scales.

Nathalie MESMER-DUDONS is an assistant Ingenieur specialized in methods of light and electronic microscopy in marine organisms. She has been titular of professional licence in Electronic Microscopy and Cellular Cultures at the university Bordeaux 1 since 1990.

Patrice GONZALEZ received his Ph.D. in molecular biology and genetics at the University of Bordeaux 2 in 1999. He is currently researcher at the French National Center for Scientific Research at the marine station of Arcachon. His research focuses on the molecular and genetic effects of metallic pollution on aquatic organisms and their adaptative response.

Stéphane MORNET received his Ph.D. in physico-chemistry of condensed matter at the University Bordeaux 1 in 2002. He is currently researcher at the Institute of Condensed Matter Chemistry. At the interface of chemistry and biology, his research focuses on the synthesis of magnetic, metallic and luminescent nanoparticles, their surface functionalization and conjugation with biomolecules for imaging and therapy purposes.

References

1   J.F. Hochepied and V. Guyot-Ferréol, www-ep.ensmp.fr/scpi/PubliSCPI/nanocosmetique.pdf, 2007

2   A. Chatterjee, A. Priyam, S.C. Bhattacharya and A. Saha, *Journal of luminescence*, 2007, **126** (2), 764-770

3   B.D. Chithrani, A.A. Ghazani and W.C. Chan, *Nanoletters*, 2006, **6** (4), 662-668

4   C.W. Corti, R.J. Holliday and D.T. Thompson, World Gold Council, London, 2004

5   B.M. Rothen-Rutishauser, S. Schürch, B. Haenni, N. Kapp and P. Gehr, *Environnemental Sciences and Technologies*, 2006, **40**, 4353-4359

6   R. Russell and R. Cresanti, Nanoscale science, engineering, and technology subcommittee, 2006

7   B. Merchant, *Biologicals*, 1998, **26**, 49-59

8   Z.P. Xu, Q.H. Zeng, G.Q. Lu and A.B. Yu, *Chemical Engineering Science*, 2005, **61**, 1027-1040

9   E. Connor, J. Mwamuka, A. Gole, C.J. Murphy and M.D. Wyatt, *Small*, 2005, **1** (3), 325-327

10 R. Shukla, V. Bansal, M. Chaudhary, A. Basu, R.R. Bhonde and M. Sastry, *Langmuir*, 2005, **21**, 10644-10654

11 M. Baudrimont, S. Andres, J. Metivaud, Y. Lapaquellerie, F. Ribeyre, N. Maillet, C. Latouche and A. Boudou, *Environmental Toxicology and Chemistry*, 1999, **18**, 2472-2477

12 M. Baudrimont, S. Andres, G. Durrieu and A. Boudou, *Aquatic Toxicology*, 2003, **63** (2), 89-102

13 D. Tran, Ecole doctorale des Sciences du vivant, Géosciences et Sciences de l'Environnement, Université Bordeaux I, 2001

14 P-E. Olsson and P. G. Kling, *Comparative Biochemistry and Physiology*, 2000, **126 A**, S1-S163

15 J. Kimling, M. Maier, B. Okenve, V. Kotaidis, H. Ballot and A. Plech, *Journal of Physic and Chemical Biology*, 2006, **110**, 15700-15707

16 D.M. John, B.A. Whitton and A.J. Brook, Cambridge University Press, 2002, 287-612

17 J. Mouthon, *Basteria*, 1981, **45**, 109-116

18 J. Schäfer, G. Blanc, S. Audry, D. Cossa and C. Bossy, *Applied Geochemistry*, 2006, **21** (3), 515-527

19 A. Legeay, M. Achard-Joris, M. Baudrimont, J.C. Massabuau and J.P. Bourdineaud, *Aquatic Toxicology*, 2005, **74**, 242–253

20 J.D. Pickett-Heaps and L.A. Staehelin, *Journal of Phycology*, 1975, **11** (2), 186-202

21 C.M. Goodman, C.D. McCusker, T. Yilmaz and V.M. Rotello, *Bioconjugate Chemistry*, 2004, **15**, 897-900

22 B. Allard, M.N. Rager and J. Templier, *Organic Geochemistry*, 2002, **33**, 789-801

23 G. Corre and C. Largeau, Université Paris VI, 1998

24 C. Bastien, Université du Québec à Chicoutimi, 1986

25 X. Shi, S. Wang, H. Sun and J.R. Baker, *Soft Matter*, 2007, **3**, 71-74

26 D. Shenoy, W. Fu, J. Li, C. Crasto, G. Jones, C. Dimarzio, S. Sridhar and M. Amiji, *International Journal of Nanamedicine*, 2006, **1** (1), 51-58

27 C. Fruijtier-Pölloth, *Toxicology*, 2005, **214**, 1-38

28 S. Andres, Université Paul Sabatier de Toulouse, 1997

29 A.W. Decho and S.N. Luoma, *Limnological Oceanography*, 1996, **41**, 568-572

30 M.L. Vidal, A. Bassères and J.F. Narbonne, *Comparative Biochemistry and Physiology*, 2002, **131** C, 133-151

31 P. Gonzalez, M. Baudrimont, A. Boudou and J.P. Bourdineaud, *Biometals*, 2006, **19**, 225-235

32 J. Chan, Z. Huang, M.E. Merrifield, M.T. Salgado and M.J. Stillman, *Coordinated Chemistry Revue*, 2002, **233-234**, 319-339

33 R. Heuchel, F. Ratke, O.Georgiev, M. Stark, M. Aguet and W. Schaffner, *EMBO Journal*, 1994, **13**, 2870-2875

34 S. Praharaj, S. Panigrahi, S. Basu, S. Pande, S. Jana, S. Kumar-Ghosh and T. Pal, *Journal of Photochemistry and Photobiology A: Chemistry*, doi:10.1016/j.jphotochem.2006.10.019

35 V. Marie, M. Baudrimont and A. Boudou, *Chemosphere*, 2006, **65**, 609-617

36 Y. Pan, S. Neuss, A. Leifert, M. Fischler, F. Wen, U. Simon, G. Schmid, W. Brandau and W. Jahnen-Dechent, *Small*, 2007, **3** (11), 1941-1949

37 W.H. De Jong, W.I. Hagens, P. Krystek, M.C. Burger, A.J.A.M. Sips and R.E. Geertsma, *Biomaterials*, 2008, **29**, 1912-1919